The following resources related to this article are available online at
www.sciencemag.org (this infomation is current as of November 18, 2010):

Updated information and services, including high-resolution figures, can be found in the online version of this article at:
http://www.sciencemag.org/content/327/5961/72.full.html

Supporting Online Material can be found at:
http://www.sciencemag.org/content/suppl/2009/12/29/327.5961.72.DC1.html

A list of selected additional articles on the Science Web sites **related to this article** can be found at:
http://www.sciencemag.org/content/327/5961/72.full.html#related

This article **cites 17 articles**, 4 of which can be accessed free:
http://www.sciencemag.org/content/327/5961/72.full.html#ref-list-1

This article has been **cited by** 3 article(s) on the ISI Web of Science

This article has been **cited by** 1 articles hosted by HighWire Press; see:
http://www.sciencemag.org/content/327/5961/72.full.html#related-urls

This article appears in the following **subject collections:**
Chemistry
http://www.sciencemag.org/cgi/collection/chemistry

still contain oxygen, and the only way to completely deoxygenate them is by using a second reactor operating in the organic phase or a high-temperature vapor phase hydrotreatment.

With solid-stabilized emulsions, a continuous process could be designed in which the two homogeneous phases coexist with the emulsion in a layered configuration: oil/emulsion/water. One can achieve full conversion on both sides of the emulsion followed by constant removal of oil-soluble products from the top layer and water-soluble products from the bottom layer while the reaction keeps occurring in the emulsion.

Our results highlight the preliminary applications of solid catalysts localized at the interface between two liquid phases. We anticipate that tailoring such emulsion-stabilizing solids with additional catalytic functional groups will facilitate a broad range of reactions.

References and Notes

1. C. M. Starks, *J. Am. Chem. Soc.* **93**, 195 (1971).
2. G. W. Huber, S. Iborra, A. Corma, *Chem. Rev.* **106**, 4044 (2006).
3. G. W. Huber, J. A. Dumesic, *Catal. Today* **111**, 119 (2006).
4. L. L. Dai, R. Sharma, C.-Y. Wu, *Langmuir* **21**, 2641 (2005).
5. G. M. Whitesides, B. Grzybowski, *Science* **295**, 2418 (2002).
6. A. D. Dinsmore et al., *Science* **298**, 1006 (2002).
7. B. P. Binks, S. O. Lumsdon, *Langmuir* **16**, 8622 (2000).
8. B. P. Binks, *Curr. Op. in Coll. and Interf. Sci.* **7**, 21 (2002).
9. B. P. Binks, C. P. Whitby, *Langmuir* **20**, 1130 (2004).
10. B. P. Binks, J. Philip, J. A. Rodrigues, *Langmuir* **21**, 3296 (2005).
11. R. K. Wang et al., *J. Am. Chem. Soc.* **130**, 14721 (2008).
12. D. E. Resasco et al., *J. Nanopart. Res.* **4**, 131 (2002).
13. M. Shen, D. E. Resasco, *Langmuir* **25**, 10843 (2009).
14. Materials and methods are available as supporting material on *Science* Online.
15. J. P. Brunelle, *Pure Appl. Chem.* **50**, 1211 (1978).
16. J. R. Regalbuto et al., *J. Catal.* **184**, 335 (1999).
17. S. Lambert et al., *J. Catal.* **261**, 23 (2009).
18. D. C. Elliott, *Energy Fuels* **21**, 1792 (2007).
19. C. Zhao, Y. Kou, A. A. Lemonidou, X. Li, J. A. Lercher, *Angew. Chem. Int. Ed.* **48**, 3987 (2009).
20. C. Saizjimenez, J. W. Deleeuw, *Org. Geochem.* **10**, 869 (1986).
21. D. Mohan, C. U. Pittman Jr., P. H. Steele, *Energy Fuels* **20**, 848 (2006).
22. R. Brückner, in *Advanced Organic Chemistry: Reaction Mechanisms* (Academic Press, New York, 2002), pp. 283–285.
23. N. Y. Chen, W. W. Kaeding, F. G. Dwyer, *J. Am. Chem. Soc.* **101**, 6783 (1979).
24. E. Iglesia, *Appl. Catal. Gen.* **161**, 59 (1997).
25. R. M. West, Z. Y. Liu, M. Peter, J. A. Dumesic, *Chem. Sus. Chem.* **1**, 417 (2008).
26. D. A. Simonetti, J. A. Dumesic, *Chem. Sus. Chem.* **1**, 725 (2008).
27. G. W. Huber, J. N. Chheda, C. J. Barrett, J. A. Dumesic, *Science* **308**, 1446 (2005).
28. This research was supported by the Oklahoma Secretary of Energy and the Oklahoma Bioenergy Center. Partial support from the U.S. Department of Energy is gratefully acknowledged.

Unveiling the Transient Template in the Self-Assembly of a Molecular Oxide Nanowheel
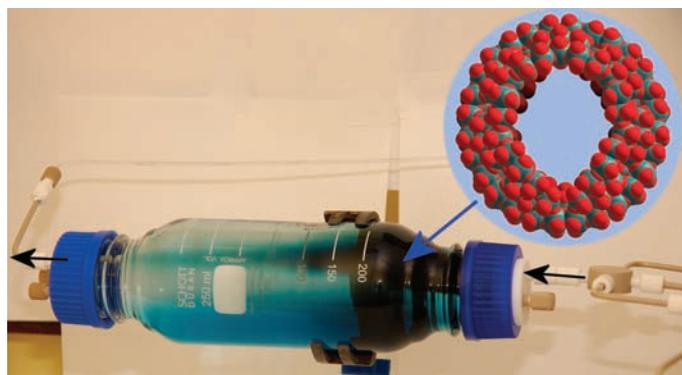
Haralampos N. Miras,[1] Geoffrey J. T. Cooper,[1] De-Liang Long,[1] Hartmut Bögge,[2] Achim Müller,[2] Carsten Streb,[1] Leroy Cronin[1]*

Self-assembly has proven a powerful means of preparing structurally intricate nanomaterials, but the mechanism is often masked by the common one-pot mixing procedure. We employed a flow system to study the steps underlying assembly of a previously characterized molybdenum oxide wheel 3.6 nanometers in diameter. We observed crystallization of an intermediate structure in which a central {Mo$_{36}$} cluster appears to template the assembly of the surrounding {Mo$_{150}$} wheel. The transient nature of the template is demonstrated by its ejection after the wheel is reduced to its final electronic state. The template's role in the self-assembly mechanism is further confirmed by the deliberate addition of the template to the reaction mixture, which greatly accelerates the assembly time of the {Mo$_{150}$} wheel and increases the yield.

The bottom-up self-assembly of large inorganic architectures is a key synthetic route for the preparation of a whole range of systems from cages (*1–3*) to metal organic frameworks (*4*, *5*) and the formation of macrocycles (*6*) from comparatively simple small molecule building blocks. In these systems the building blocks, and the underlying self-assembly processes, are understood to such a high degree that many complex and intricate structures can be designed from first principles, and the resulting architectures can even be postsynthetically modified (*7*). However, when nanostructures in the 2- to 10-nm range are targeted (e.g., metallic nanoparticles and quantum dots), the self-assembly can be critically limited by the high number of degrees of freedom, and it is not trivial to target narrow size distributions. In contrast, in supramolecular chemistry, molecular templates have been successfully employed as external directors in the design of receptors (*3*, *8–10*) and can facilitate the assembly of molecular nanostructures that are intrinsically monodisperse. Spectacular assembly control has been demonstrated by deliberate targeting and synthesis of templates that by design enable the formation of a predetermined structure, yet it is difficult to design large structures (*2*). The discovery of a similar templating strategy for the reliable fabrication of 2- to 10-nm molecular nanoparticles would revolutionize the synthesis and applications of molecular materials in the same way that templated synthesis has revolutionized the field of organic macrocyclic synthesis over the past 40 years.

In recent years, Müller and co-workers reported the solution-phase assembly of a family

[1]WestCHEM, Department of Chemistry, The University of Glasgow, Glasgow, G12 8QQ, UK. [2]Fakultät für Chemie, Universität Bielefeld, Postfach 100131, 33501 Bielefeld, Germany.

*To whom correspondence should be addressed. E-mail: L.Cronin@chem.gla.ac.uk

Fig. 1. A photograph of the flow-reactor system showing the blue reduction wavefront gradient formed within the vessel during the assembly of compound **1** (the reduced region is blue, and the more oxidized region is pale to clear). The structure of the {Mo$_{150}$} wheel present in compound **1** is shown in space-filling ball-and-stick mode. Mo ions are green spheres; O ligands are red spheres.

of nanoscale metal-oxide rings composed of 140 to 154 molybdenum centers by reduction of an acidic (pH = 1 to 3) molybdate solution, which have a range of interesting physical and chemical properties arising from their molecular nature, nanoscale size, and electronic distribution (11–15). These rings crystallized either as ordered chain/layer assemblies or discrete molecules. Diffraction analysis revealed that each individual ring appeared to have assembled from several classes of discrete $[Mo_xO_y]$ building blocks, most commonly $\{Mo_2\}$, $\{(Mo)Mo_5\}$, and $\{Mo_8\}$ bonded together through oxo-bridges to form $\{Mo_{154-x}\}$ ($x = 0$ to 14) rings 3.6 nm in diameter. We hypothesized that some sort of internal templating must have played a role in such an intricate assembly process, but the deceptively simple reaction conditions have so far effectively concealed the enormous complexity involved in this self-assembly process. We probed the self-assembly of the molybdenum blue (MB) nanoparticles using a dynamic synthetic procedure in a flow system that enabled real-time adjustment of the three input variables (pH, concentration of molybdate, and reducing agent) controlling the synthesis of the molecular nanosized-wheels (Fig. 1).

By using a flow system, rather than combining all reagents at once in a single flask ("one pot"), we were able to maintain an off-equilibrium reaction system in which we carefully controlled the degree of reduction of the polyoxomolybdate clusters. To achieve this reaction state, screening

of the synthetic parameters—for example, the concentration of molybdate, reducing agent, pH, and ionic strength—was required to determine the correct flow rate. If the flow rate was too low, then the reduced molybdate would be produced in such low concentration that crystallization would not occur and the reduced molybdate within the system would be reoxidized by oxygen over a period of days (i.e., the solution would become colorless). If the flow rate was too high, then the whole system would become over-reduced and no gradient between the reduced and oxidized regions would be set up on a time scale that would allow crystallization (i.e., the solution would become uniformly dark blue).

However, after optimizing the flow system, we were also able to isolate and trap, by crystallization, a key intermediate in the assembly of wheel-type MB nanocluster whereby single crystals were formed in the flow reactor and isolated by halting the flow and filtering the product after a given run time of 2 to 3 days. Specifically, we characterized a hollow $\{Mo_{150}\}$ wheel that hosts a $\{Mo_{36}\}$ cluster that is bound to the central cavity of the ring species by charge-balancing sodium cations, and in the solid state the wheel itself is weakly covalently linked through 5 oxo-bridges to chains (16). This host-guest complex shows features indicative of an intermediate electronic and structural state, and we postulate that the $\{Mo_{36}\}$ cluster acts as the key template in the formation of the MB ring. We isolated the host-guest complex as the crystalline compound 1, $Na_{22}[Mo^{VI}_{36}O_{112}(H_2O)_{16}] \subset [Mo^{VI}_{130}Mo^{V}_{20}O_{442}(OH)_{10}(H_2O)_{61}] \cdot 180H_2O \equiv Na_{22} \cdot 1a \cdot 180H_2O$ in a gram yield of 4.5 g, 17.4% by the reduction of an aqueous acidic solution of $Na_2MoO_4 \cdot 2H_2O$ with $Na_2S_2O_4$ under continuous addition of HNO_3, and we were able to determine the formula of the host-guest compound

unambiguously using many lines of investigation (16). The key to this discovery was the use of nitric acid in the flow system in a dual role as a proton source and an oxidant leading to incomplete reduction of the wheel. The archetypal wheel $\{Mo_{154}\}$ has 14 two-electron reduced compartments (i.e., a total of 28 4d electrons), but in the present case, only 10 of the 14 compartments are two-electron reduced, rendering the overall intermediate wheel 20-electron reduced (as confirmed by a combination of structural studies, chemical analysis, redox titration, and solution UV-VIS spectroscopy). Compound 1 crystallizes in the space group $C2/m$ and has a large unit cell with a volume of 41,734 $Å^3$. The corresponding formula was determined by elemental analyses, single-crystal x-ray structure analysis, bond valence sum calculations, redox titrations, and thermogravimetry (16). Structural analysis revealed that the $\{Mo_{150}\}$ wheel features an ellipsoidal central cavity of ~2.6 × 1.8 nm in which a $\{Mo_{36}\}$ unit resides. The principal axis of the $\{Mo_{36}\}$ template is tilted by 38.5° with respect to the main wheel plane and is linked to the $\{Mo_{150}\}$ wheel through sodium cation bridges that reduce the electrostatic repulsion between the two negatively charged constituents (Fig. 2), and the binding of the guest is also stabilized by hydrogen-bonded interactions to the host. The $\{Mo_{150}\}$ wheel in 1a consists of 14 $\{Mo_8\}$-type pentagonal building units (blue, Fig. 2) which are linked along the inner rim of the wheel by 12 $\{Mo_2\}$ linker units (red, Fig. 2), as opposed to the 14 $\{Mo_2\}$ units present in the archetypal wheel (4, 15), and connected by 14 $\{Mo_1\}$ groups along the central equatorial region of the structure (yellow, Fig. 2), so that the wheel-type cluster in 1a can be formulated as $\{Mo_{150}\} = (\{Mo_1\}_{14}\{Mo_2\}_{12}\{Mo_8\}_{14})$; the decrease in the number of the $\{Mo_2\}$ building blocks in MB

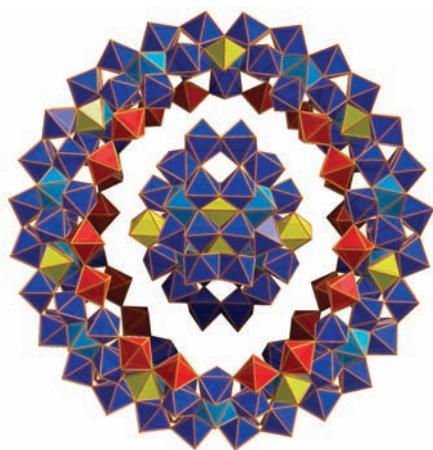**Fig. 2.** A polyhedral representation of the nanoscale $\{Mo_{36}\} \subset \{Mo_{150}\}$ wheel as part of the chain 1a [for linking details, see fig. S3 and the chains with pure wheels in (19)]. Sodium cations have been omitted for clarity, although there are ~22 positions on the inner side of the ring where sodium resides, of which 12 directly bridge the template to the outer ring. The host and the guest are also connected by a series of hydrogen bonds. The polyhedral building blocks are colored as follows: $\{Mo_1\}$, yellow; $\{Mo_2\}$, red; $\{Mo_8\}$, blue with a light blue pentagonal central group.
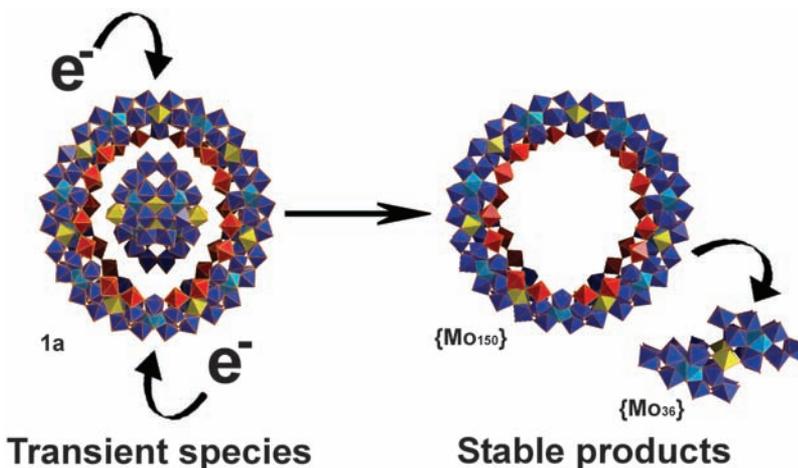

Fig. 3. Representation of the expulsion process. The addition of eight additional electrons increases the repulsion between the ring and the template, leading to the expulsion of the $\{Mo_{36}\}$ unit, that is, a separation into a pure $\{Mo_{150}\}$ phase and a pure $\{Mo_{36}\}$ phase (both isolated as crystalline solids). Color scheme as in Fig. 2.
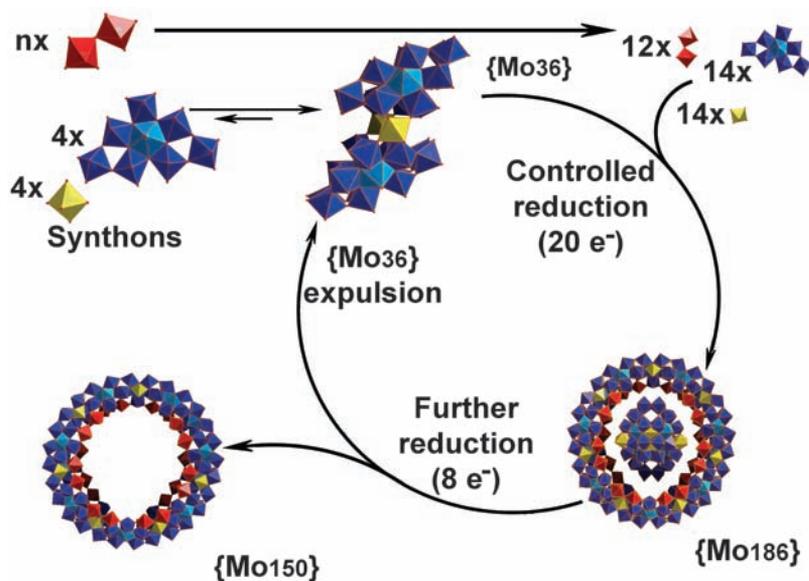
Fig. 4. Conceptual representation of the MB assembly showing the building block "synthons" (which are assigned on the basis of structural considerations) that form the template complex. The $\{Mo_{36}\}$, $\{Mo_{150}\}$, and $\{Mo_{36}\subset Mo_{150}\}$ complexes have each been isolated separately. Continuous flow-reaction conditions, along with a finely tuned reducing environment, are required to trap the template complex. Color scheme as in Fig. 2.

wheels has been previously documented as the formation of "defect" sites (*17–19*). The $\{Mo_{150}\}$ wheel in **1a** can be geometrically related to the ring-shaped $\{Mo_{154}\} \equiv [Mo_{154}O_{462}H_{14}(H_2O)_{70}]^{14-}$ cluster archetype (*11,14*). According to the classification devised to describe these MB ring–type architectures (*14, 15, 17*), the formula of the $\{Mo_{150}\}$ wheel in **1a** can be approximately expressed in terms of the building blocks $[\{Mo_2\}_{12}\{Mo_8\}_{14}\{Mo_1\}_{14}]^{14-}$, and the overall formula is $[Mo^{VI}_{130}Mo^{V}_{20}O_{442}(OH)_{10}(H_2O)_{61}]^{14-}$ (*20*). The formula was deduced with the help of bond valence sum analysis on the structural data (distinguishing between the reduced and non-reduced Mo centers and between protonated and nonprotonated O atoms), and this was confirmed chemically using redox titrations and chemical analysis [see (*16*) for a detailed analysis of the wheel structure].

The transient nature of the wheel-template complex is supported by comparative reactivity studies and is reflected in its geometric and electronic structure. In contrast to the archetypal, highly symmetrical D_{7d} $\{Mo_{154}\}$ MB wheel, the $\{Mo_{150}\}$ wheel in **1a** is elliptical with maximum outer and inner ring diameters of ~3.6 and 2.6 nm, and minimum outer and inner ring diameters of ~3.5 and 1.8 nm (Fig. 3). This ellipsoidal structure appears to be a result of the central $\{Mo_{36}\}$ template: Comparison of the ratio between the maximum and minimum cluster dimensions for both the wheel and the template ($R_{l/s}$) shows a close match between $\{Mo_{36}\}$ ($R_{l/s} = 1.42$) and the inner ring of $\{Mo_{150}\}$ ($R_{l/s} = 1.44$). Another striking feature of the $\{Mo_{36}\subset Mo_{150}\}$ template-wheel as-

sembly is the nonuniform delocalization of 20 4d electrons over the molybdenum centers. Bond valence sum calculations (*16*) for the Mo centers of the $\{Mo_{150}\}$ wheel show that the Mo centers close to the two defect sites at the most compressed sections of the wheel are fully oxidized (+6), whereas those in the least compressed region are reduced to +5. This electronic anisotropy stands in contrast to the 28-electron reduced $\{Mo_{154-X}\}$ rings, where the electrons are delocalized more symmetrically over the cluster surface (*14, 15, 18*). The intermediate 20-electron reduced MB wheel clearly favors the inclusion of the anionic $\{Mo_{36}\}$ template more than the 28-electron reduced $\{Mo_{154-X}\}$ systems. This observation is confirmed by its further reduction in solution upon replacing nitric acid with HCl in the flow reactor, which results in the expulsion of the template and the crystallization of two separate crystalline phases, including the empty, fully symmetric, and 28-fold reduced $\{Mo_{150}\}$ wheel and the $\{Mo_{36}\}$ template (Fig. 3).

On the basis of these data, we postulate that the overall mechanism underpinning the formation of the $\{Mo_{154-x}\}$ family involves the $\{Mo_{36}\}$ cluster as a structure-directing template. In keeping with this hypothesis, the $\{Mo_{36}\}$ cluster is well known to form spontaneously in acidified molybdate solutions in the absence of reducing agent. As a result, we can formulate the mechanism (Fig. 4).

To test this hypothesis, we compared the time necessary to synthesize the wheel nanoparticles under static conditions, where the molybdate, reducing agent, and acid were added simulta-

neously, versus flow conditions in which $\{Mo_{36}\}$ was added to a reduced molybdate solution. In the latter case, crystallization started after only 6 to 8 hours, yielding gram quantities of the wheel-based MB nanoparticles within 1 day. The static system required between 3 and 5 days (after crystallization commenced) to produce the same amount of material as isolated from the flow system over the period of 1 day.

Our results illustrate how a bottom-up assembly process can be used to rapidly obtain gram quantities of a nanomaterial with well-defined size, shape, and composition. Furthermore, the use of a flow reactor proved to be a powerful tool in unveiling the mechanism of assembly of the $\{Mo_{154-x}\}$ nanowheel family, and we envision the technique emerging as a versatile means of generating off-equilibrium reaction conditions for mechanistic studies of self-assembly processes.

References and Notes

1. S. Sato *et al.*, *Science* **313**, 1273 (2006).
2. P. Mal, B. Breiner, K. Rissanen, J. R. Nitschke, *Science* **324**, 1697 (2009).
3. P. N. W. Baxter, in *Comprehensive Supramolecular Chemistry*, Vol. 9, J. L. Atwood, J. E. D. Davies, D. D. MacNicol, F. Vögtle, Eds. (Pergamon/Elsevier, New York, 1996), pp. 165–211.
4. K. Chae *et al.*, *Nature* **427**, 523 (2004).
5. R. Matsuda *et al.*, *Nature* **436**, 238 (2005).
6. B. J. Holliday, C. A. Mirkin, *Angew. Chem. Int. Ed.* **40**, 2022 (2001).
7. K. L. Mulfort, O. K. Farha, C. Stern, A. A. Sarjeaut, J. T. Hupp, *J. Am. Chem. Soc.* **131**, 3866 (2009).
8. J. D. Badjic, V. Balzani, A. Credi, S. Silvi, J. F. Stoddart, *Science* **303**, 1845 (2004).
9. D. J. Cram, *Nature* **356**, 29 (1992).
10. J.-M. Lehn, *Science* **227**, 849 (1985).
11. A. Müller *et al.*, *Angew. Chem. Int. Ed. Engl.* **34**, 2122 (1995).
12. A. Müller, S. Roy, *Coord. Chem. Rev.* **245**, 153 (2003).
13. D.-L. Long, E. Burkholder, L. Cronin, *Chem. Soc. Rev.* **36**, 105 (2007).
14. A. Müller, C. Serain, *Acc. Chem. Res.* **33**, 2 (2000).
15. A. Müller *et al.*, *Chem. Eur. J.* **5**, 1496 (1999).
16. Materials and methods are available as supporting material on *Science* Online.
17. A. Müller *et al.*, *Z. Anorg. Allg. Chem.* **625**, 1187 (1999).
18. S. Shishido, T. Ozeki, *J. Am. Chem. Soc.* **130**, 10588 (2008).
19. A. Müller *et al.*, *Angew. Chem. Int. Ed. Engl.* **36**, 484 (1997).
20. Crystal structure parameters as a CIF file are available from CrysDATA@FIZ-Karlsruhe.de (CSD reference 380343). We thank the UK Engineering and Physical Sciences Research Council (EPSRC), The University of Glasgow, and WestCHEM for funding.